Results in Physics 9 (2018) 692–697

Contents lists available at ScienceDirect

Results in Physics

journal homepage: www.journals.elsevier.com/results-in-physics

Measurement of energy transitions for the decay radiations of ^{75}Ge and ^{69}Ge in a high purity germanium detector

Güral Aydın [a,*], Metin Usta [a], Adem Oktay [b,c]

[a] Department of Physics, Mustafa Kemal University, TR-31034 Hatay, Turkey
[b] Department of Physics, Osmaniye Korkut Ata University, TR-80000 Osmaniye, Turkey
[c] Altıncag Primary School, TR-31034 Hatay, Turkey

ARTICLE INFO

Article history:
Received 18 September 2017
Received in revised form 10 January 2018
Accepted 11 January 2018
Available online 2 February 2018

Keywords:
Photoactivation
Energy transitions
Photonuclear reactions
Clinic linac

ABSTRACT

Photoactivation experiments have a wide range of application areas in nuclear, particle physics, and medical physics such as measuring energy levels and half-lifes of nuclei, experiments for understanding imaging methods in medicine, isotope production for patient treatment, radiation security and transportation, radiation therapy, and astrophysics processes. In this study, some energy transition values of the decay radiations of ^{75}Ge and ^{69}Ge, which are the products of photonuclear reactions (γ, n) with germanium isotopes (^{75}Ge and ^{69}Ge), were measured. The gamma spectrum as a result of atomic transitions were analysed by using a high purity semiconductor germanium detector and the energy transition values which are presented here were compared with the ones which are the best in literature. It was observed that the results presented are in agreement with literature in error range and some results have better precisions.

Introduction

The data which are obtained as results of photonuclear reactions could be used for different purposes such as determining half-life of atomic nuclei [1–6], measuring energy levels of nuclei and study of decay products [7–10], analysis of required designs for radiation security and transportation, applications in radiation therapy and dose calculations [11–15], determining energy of photons produced in linear accelerators [16], isotope production [17,18], nuclear waste transformation, analysis of atomic nuclei which is essential for astrophysics and nucleosynthesis process [19–26], analysis of fission and fusion reactions [27] and activation analysis [28–31]. The information about what energy levels nuclei have and how long nuclei stay in certain energy levels is important to know about nuclear structures. The aim of this study is to determine some energy transition values of interested and clearly analyzed decay radiations belonging to Germanium isotopes as a result of photon induced reactions even with better precision compared to data presented in literature. In the rest of this section, first some historical review belonging to measurements of energy transition values in several nuclei are given and after that our experiment and analysis technique are briefly explained.

The experimental studies to determine energy levels and to measure half-life of nuclei and the study of decay products have also been performed with different methods rather than photoactivation such as neutron and proton induced reactions. For example, the energy levels of ^{31}As and ^{19}Ne were determined with the reactions of ^{32}S$(n,d)^{31}$P and ^{19}F$(p,n)^{19}$Ne, respectively [32]. The energy levels of ^{90}Y nucleus were measured with the reaction of deuteron-proton (d,p) [33]. The energy levels of ^{47}V and ^{49}V were determined by using the proton-alpha (p,α) reaction [34]. Krane studied the decays of ^{72}Ga with the neutron bombardment [35]. In the study which was performed by Siegel and Glendenin, the half-life was assigned for ^{73}Ga [5]. Ythier and his colleagues, the half-life for ^{73}Ga and two beta branchings were found with the bombardment of neutron and deuteron [36]. Moreover, some other studies carried out with developing technologies for measuring energy levels are listed in the references of [37–41].

The presented study is an example of using clinic linear accelerator (cLinac) in a nuclear physics experiment. In this study, a cLinac was used as a photon source for the photonuclear interaction. It has already been shown that cLinacs could be used for photoactivation experiments by providing required photon intensity [42] right along with electron linear accelerators [43–45]. The required photons were obtained with a cLinac, directed to Germanium isotopes and some nuclear energy transitions belonging to products of germanium isotopes were determined. The other aspect of this study is that the results presented here were obtained with an analysis technique which has offline nature. That is, the results were extracted from complete data which were collected during

* Corresponding author.
E-mail address: gaydin@mku.edu.tr (G. Aydın).

https://doi.org/10.1016/j.rinp.2018.01.026
2211-3797/

the experiment without any constraints. That means prompt energies are not considered but analysis was carried out over accumulated data. The analysis details are explained in the analysis section of this report.

Theory and experiment

In this study, the observed and analyzed energy transitions belonging to (γ, n) photonuclear reactions on Germanium isotopes are shown in Eqs. (1) and (2):

$$^{70}\mathrm{Ge} + \gamma \rightarrow {}^{69}\mathrm{Ge} + n \quad (1)$$

$$^{76}\mathrm{Ge} + \gamma \rightarrow {}^{75}\mathrm{Ge} + n \quad (2)$$

^{69}Ge and ^{75}Ge are called as the product nuclei of the germanium isotopes after gamma irradiation. These products decay and then excited daughter nuclei (^{69}Ga* and ^{75}As*) are produced. The decay processes are given in Eqs. (3) and (4):

$$^{69}\mathrm{Ge} \rightarrow {}^{69}\mathrm{Ga}^{*} + e^{-} + \bar{\nu}_e \quad (3)$$

$$^{75}\mathrm{Ge} \rightarrow {}^{75}\mathrm{As}^{*} + e^{-} + \bar{\nu}_e \quad (4)$$

Then, these excited daughter nuclei emit photons as a result of atomic transitions which will be detected in our high purity germanium detector. These processes are illustrated in Eqs. (5) and (6):

$$^{69}\mathrm{Ga}^{*} \rightarrow {}^{69}\mathrm{Ga} + \gamma \quad (5)$$

$$^{75}\mathrm{As}^{*} \rightarrow {}^{75}\mathrm{As} + \gamma \quad (6)$$

The bremsstrahlung photons used in activation processes were obtained from a Philips (Elekta TM Synergy) clinic electron linear accelerator which is used basically for medical purposes. The technical documentation about the clinical linac can be found at [46]. The primary electrons were produced by a gun whose energy is 50 keV and has the pulse repetition frequency of 400 Hz. The accelerator reached a peak power of about 5 MW and provided 4, 6 and 18 MeV endpoint bremsstrahlung energy spectrum with tungsten element as bremsstrahlung converter. 0.3 mm thick tungsten target was used as a converter target.

The radioactivity measurements were performed with a p-type, coaxial, and high purity germanium detector (HPGe). The detector has a cooling with electricity. The brand of the detector is AMATEK ORTEC (GEM40P483) and its relative efficiency is 40%. The detector has FWHM values of 768 eV and 1.85 keV at 122 keV peak of ^{57}Co radioisotope and at 1332 keV peak of ^{60}Co radioisotope, respectively [47]. The HPGe detector was connected to a computer and NIM (Nuclear Instrumentation Module) which is consists of a power supply, spectroscopy amplifier and analog to digital converter which all belong to the company of ORTEC. The detector are divided into 16,830 channels with about 0.18 keV energy range that each channel covers. It was saved in a 10 cm thick lead shield whose inner side was coated with 2 mm thick copper layer to avoid X-rays which could be caused by the lead shield.

The germanium sample is 10 gr GeO_2 powder with 99.99% purity which was formed as a pill by squeezing it. The sample was placed 58 cm away from the source of clinic accelerator (tungsten target) and was beamed out with bremsstrahlung photons which have 18 MeV endpoint energy. The irradiation time for germanium sample was about half an hour and the delivered dose are estimated as 5 Gy/min corresponding about 1011 electron/s. This gives 5×105 photon/(MeV cm^2 s). The sample was located in front of the detector nearly 10 min later after it was beamed out in clinic accelerator and the counting process took place for 75 h. The records were taken for different time periods (9, 90, 900, 8775 s spectrum records). Besides, counts were obtained for calibration sources immediately before and after the counting process of our interested germanium sample to measure changes during our original counting process. These calibration processes will be mentioned in the text as before and after count processes. Various point and composite calibration sources, whose well-known gamma-ray energies are between 47 and 1837 keV, were provided for energy calibration from Cekmece Nuclear Research Center (IAEA 1364-43-2).

Analysis

The last file in the spectrum records included all photopeaks for germanium isotopes which are given in three parts with Figs. 1–3. The counting process was short for point sources and only one file was recorded for each source of ^{133}Ba, ^{109}Cd, ^{57}Co, ^{60}Co, ^{137}Cs, ^{54}Mn, ^{22}Na, ^{228}*Ac*, ^{214}Pb, ^{214}Bi, and ^{208}Tl. All photopeaks in the spectrums were fitted with gaussian, skewed gaussian and a smoothed step function by using the RadWare analysis program [48]. The fit

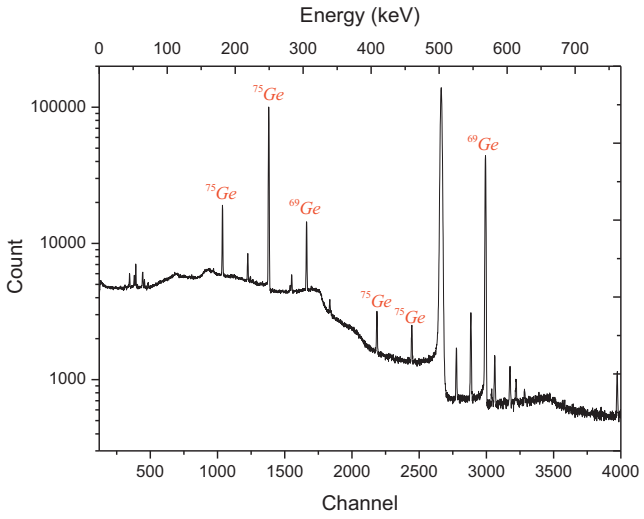

Fig. 1. Photopeak spectrum of Germanium sample hitting detector channels in the range of 0–4000.

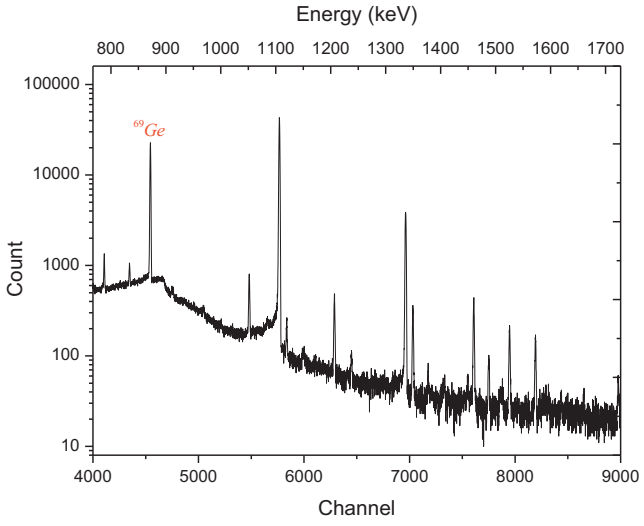

Fig. 2. Photopeak spectrum of Germanium sample hitting detector channels in the range of 4000–9000.

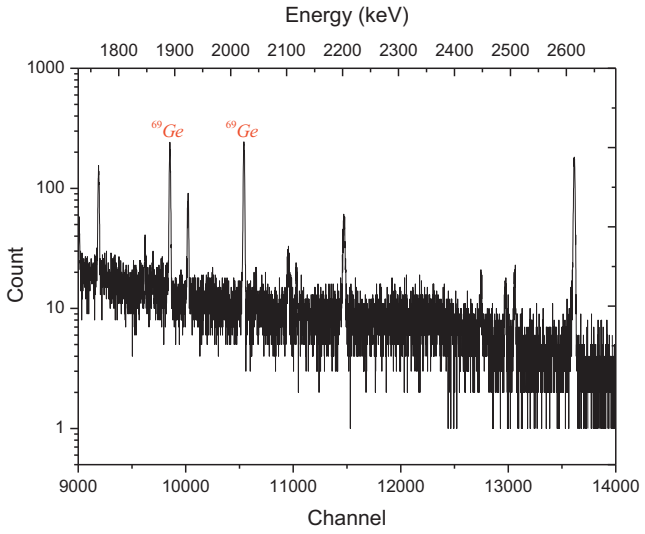

Fig. 3. Photopeak spectrum of Germanium sample hitting detector channels in the range of 9000 and 14,000.

function deals also with background estimation under the main peak. Therefore, the range of the fit must be large enough to take account background distribution before and after the main peak. In the study, the range and fit parameters was selected such a way that the chi square value was as close to 1 as possible. The best parameters estimated the background under the main peak according to the tendency of background immediately before and after the main peak. This program was developed for analysis of gamma-ray data by David Radford, Physics Division at Oak Ridge Laboratory. The fitting was performed for all photopeaks including point sources and original germanium isotopes. The fit results provided us with the center channel numbers (centroid) and their errors. The idea was to obtain polynomial formula to convert measured channel numbers to corresponding energy values. This was managed with calibration sources whose radiation energies are well-known in literature. Once a formula was determined with calibration sources, then the channel numbers found for germanium isotopes were used to obtain corresponding energy values whose decay processes are clearly separated from others. First of all, combined channel numbers for each calibration source were determined by taking the average of centroid values of the same source for before and after count processes as in Eq. (7):

$$C_c = (C_b + C_a)/2 \tag{7}$$

The errors on combined channel numbers were calculated by using standard error propagation given in Eq. (8):

$$\sigma_{C_c} = \sqrt{\left(\left(\sigma_{C_b}^2 + \sigma_{C_a}^2 + (C_b - C_c)^2 + (C_a - C_c)^2\right)/2\right)} \tag{8}$$

Here, C_c, C_b, C_a, σ_{c_b}, σ_{c_a} refers to combined channel number, channel number of before count, channel number of after count, total errors on channel numbers for before and after counts, respectively. The resulting values are shown in Table 1 with the literature values of corresponding energy values [49–59]. The combined channel numbers of calibration sources and their corresponding energy values which are best in literature were put in a 2-D scatter histogram to perform a best polynomial fit as shown in Fig. 4.

The fit results are shown in Table 2, where a_0, a_1 and a_2 are the parameters of the second order polynomial fit and cov01, cov02 and cov12 are the covariance matrix elements for the fit. In this way, we obtained the following energy formula as in Eq. (9) as a function of centroid channel numbers (ch) of photopeaks.

$$E = a_0 + a_1(ch) + a_2(ch)^2 \tag{9}$$

The error on the energy value included errors on fit parameters, covariance matrix elements [60–63] and errors on centroid channel numbers. Generally, if one takes energy equation as shown in Eq. (10), then the error on the energy value could be written as in Eq. (11) or in Eq. (12):

$$E = \sum_i^n a_i ch^i \tag{10}$$

$$\sigma_E^2 = \sum_i^n \left(\frac{\partial E}{\partial a_i}\right)^2 \sigma_{a_i}^2 + 2\sum_i^n \sum_{j>i}^n \left(\frac{\partial E}{\partial a_i}\right)\left(\frac{\partial E}{\partial a_j}\right) cov_{ij} + \left(\frac{\partial E}{\partial ch}\right)^2 \sigma_{ch}^2 \tag{11}$$

Table 1
Centroid channel numbers of photopeaks from calibration sources spectrums for measurements of before (C_b) and after (C_a) the original sample (germanium) count, combined channel numbers (C_c), errors on combined channel numbers (σ_{C_c}) and nudat values for related energy levels $(E_{NU}(keV))$.

Elements	C_b	σ_{C_b}	C_a	σ_{C_a}	C_c	σ_{C_c}	$E_{NU}(keV)$
^{133}Ba	278.4092	0.0700	279.3383	0.0632	278.8738	0.4693	53.1622
^{133}Ba	1580.2307	0.0132	1580.1599	0.0121	1580.1953	0.0376	302.3950
^{133}Ba	1857.2310	0.0078	1857.1554	0.0072	1857.1932	0.0385	356.0129
^{133}Ba	2002.3162	0.0229	2002.1321	0.0196	2002.2242	0.0945	383.8485
^{109}Cd	460.3572	0.0502	460.5771	0.0510	460.4672	0.1210	88.0336
^{57}Co	638.1111	0.0229	637.9998	0.0206	638.0555	0.0598	122.0607
^{57}Co	713.1731	0.0700	713.0144	0.0635	713.0938	0.1037	136.4736
^{60}Co	6114.1455	0.0198	6113.9600	0.0182	6114.0528	0.0947	1173.2280
^{60}Co	6943.7051	0.0218	6943.4561	0.0200	6943.5806	0.1262	1332.4920
^{137}Cs	3449.4578	0.0099	3449.2446	0.0087	3449.3512	0.1070	661.6570
^{54}Mn	4351.6851	0.0461	4350.9526	0.0492	4351.3189	0.3693	834.8480
^{22}Na	6641.8135	0.0248	6641.4492	0.0224	6641.6314	0.1837	1274.5370
^{214}Pb	1540.8563	0.0468	1539.6534	0.0280	1540.2549	0.6027	295.2228
^{214}Pb	1835.2681	0.0345	1835.9827	0.0206	1835.6254	0.3584	351.9321
^{214}Bi	3176.8098	0.0424	3176.9260	0.0267	3176.8679	0.0681	609.3200
^{214}Bi	5838.3228	0.1279	5838.0522	0.0857	5838.1875	0.1737	1120.2940
^{228}Ac	4748.2461	0.0710	4749.2515	0.0566	4748.7488	0.5068	911.2040
^{214}Bi	9193.0752	0.1684	9193.4902	0.1055	9193.2827	0.2506	1764.4910
^{208}Tl	3041.3301	0.0524	3040.1921	0.0318	3040.7611	0.5706	583.1870
^{208}Tl	13620.1924	0.1556	13620.4893	0.1038	13620.3409	0.1988	2614.5110

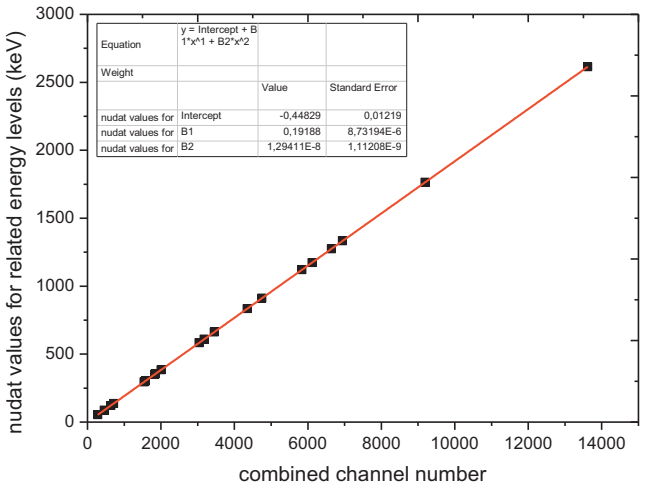

Fig. 4. Combined channel numbers for calibration point sources versus corresponding energy values taken from literature with the best values. The continuous line shows the second order polynomial fit.

Table 2
Calibration parameters for the second order polynomial fit $E = a_0 + a_1 C_c + a_2 (C_c)^2$. σ_{a_0}, σ_{a_1} and σ_{a_2} are errors on fit parameters.

Fit parameters	Values	Error(σ_{a_i})
a_0	−0.448291	0.0121913
a_1	0.191881	8.73194E−06
a_2	1.29411E−08	1.112085E−09
cov01	−9.4628E−08	–
cov02	1.07321E−11	–
cov03	−9.40348E−15	–

Table 3
Calibration parameters for the fit belonging to not the combined centroids of before and after source spectrums but to the lowest peak values among both spectrums for each sources.

Fit parameters	Values	Error(σ_{a_i})
a_0	−0.376095	0.00428854
a_1	0.191911	2.82586E−06
a_2	7.37E−08	3.66321E−10
cov01	−1.08176E−08	–
cov02	1.24075E−12	–
cov12	1.24075E−12	–

$$\sigma_E^2 = \sum_i^n \left(\frac{\partial E}{\partial a_i}\right)^2 \sigma_{a_i}^2 + 2\sum_i^n \sum_{j>i}^n \left(\frac{\partial E}{\partial a_i}\right)\left(\frac{\partial E}{\partial a_j}\right) cor_{ij} + \left(\frac{\partial E}{\partial ch}\right)^2 \sigma_{ch}^2 \quad (12)$$

where *ch* represents channel number and a_i are constants. Then, if one applies this to our energy equation of Eq. (9) and use covariance matrix elements, Eq. (13) is obtained for error calculation on energy values including statistical and systematical errors:

$$\sigma_E^2 = \sigma_{a_0}^2 + C_c^2\sigma_{a_1}^2 + C_c^4\sigma_{a_2}^2 + 2((ch)cov01 + ch^2 cov02 + ch^3 cov12) + (a_1 + 2a_2 ch)^2 \sigma_{ch}^2 \quad (13)$$

The total error is caused by several sources. The uncertainty in peak position and energy calibrations leads to statistical errors. Besides, channel drift during the experiment causes systematical errors. Since there is difference in peak positions between before and after source spectrums, the additional conservative error was considered. For this, the polynomial fit was redone by this time using not combined channel numbers of calibration spectrums but taking the lowest one among before and after counts for each sources. The new fit parameters are shown in Table 3. This did not break up linearity much but the constant changed significantly representing uncertainty of shift on peak positions during the experiment. The difference between energy values calculated with two different fit parameters was used as an additional error. The quadratic summation of both errors, which are calculated according to Eq. (13) and along with fit parameters, was the total error for each channel analysed.

Results and discussion

The photopeak results for the germanium sample count are shown in Table 4. The channel numbers from the detector (centroids), the width values of the fit functions, corresponding energy values obtained with Eq. (12), total errors, and Nuclear Data Table (nudat) values of the related energy transitions belonging to the decay radiations of ^{75}Ge and ^{69}Ge are listed [64,65]. As shown in the table, all nine results are in agreement with literature values within error range. Two energy values 198.6 keV and 264.6 keV are the same as with corresponding literature values. There is 0.02 keV difference between our measurement and literature value for the energy measured as 3.61 keV but a better error is introduced in the presented study. The literature values of 419.1 keV and 468.8 keV energies were measured as 418.8 and 468.5 keV in the presented study, respectively. These energies are nearly in agreement in error ranges but better errors were introduced in our study compared to literature ones. The 574.11 keV energy in literature with 0.10 keV error is 0.13 keV higher than the measured one with 0.11 keV error. The measured value of 871.77 keV with 0.10 keV error is 871.98 keV in literature with 0.10 keV error. The measured 1891.36 keV energy with 0.18 keV error is 0.12 keV lower than that of literature value with 0.10 keV error matching in error ranges easily but with worse error on measured site. For the last, the 2023.65 keV literature value differ with the presented value by 0.39 keV but they are in agreement by considering 0.20 keV and 0.24 keV errors. In summary, the presented experiment which has offline nature for determining energy values gives very

Table 4
The photopeak results for the germanium sample count. The channel numbers from the detector (centroid), the width values of the fit functions, corresponding energy values obtained with Eq. (12) ($E(keV)$), error on energy values (σ_E) and literature values (nudat).

Elements	Centroid	Width of the fit function	$E_{NU}(keV)$	σ_{NU}	$E(keV)$	σ_E
^{75}Ge	1037.0704	5.13	198.6	0.1	198.56	0.098
^{75}Ge	1381.1466	4.47	264.6	0.1	264.59	0.103
^{75}Ge	2184.8533	5.58	419.1	0.2	418.85	0.11
^{75}Ge	2443.7461	6.2	468.8	0.2	468.54	0.11
^{69}Ge	1662.6044	5.44	318.63	0.20	318.61	0.107
^{69}Ge	2993.0281	6.94	574.11	0.10	573.97	0.11
^{69}Ge	4544.2114	8.43	871.98	0.10	871.77	0.094
^{69}Ge	9852.7539	13.43	1891.48	0.10	1891.36	0.18
^{69}Ge	10543.2314	13.4	2023.65	0.20	2024.04	0.24

close results to literature values. Finally, in the light of our experiment results, it could be concluded that this type of analysis could also give good results in addition to the methods which have online natures.

Conclusion

In this study, a clinic linac was used producing bremsstrahlung photons with endpoint energy of 18 MeV. It could be stated that such systems could be used in nuclear physics experiments. This experiment has offline nature, so it is not considered for measuring prompt photons once they are produced. The analysis took place once all data had been collected during the experiment. The results of transition energies presented here were obtained offline by taking account of original sample count and counts from calibration source samples taken immediately before and after the original germanium counting process. It can be seen that the analysed and presented transition values agree with the corresponding literature values in error ranges. When compared with literature, some energy results are very close including errors, some are again very close and have better errors presented in this study. Finally, it could be stated that this work gives a contribution to nuclear data.

Acknowledgments

This project was supported by a Mustafa Kemal University, Turkey, Scientific Research Projects Coordinatorship with the grant of BAP-12061.

Appendix A. Supplementary material

Supplementary data associated with this article can be found, in the online version, at https://doi.org/10.1016/j.rinp.2018.01.026.

References

[1] Yoshida E et al. Half-lives of isomeric levels of 107mAg, 109mAg and 103mRh photoactivated by 60Co γ-ray irradiation. Nucl Instrum Methods Phys Res Sect A: Accelerat, Spectromet, Detect Assoc Equip 2000;449(1–2):217–20.
[2] Wen X-Q et al. Half-lives of isomeric levels of 87mSr, 111mCd, 113mIn and 115mIn activated by 60Co γ-ray irradiation. Nucl Instrum Methods Phys Res Sect A: Accelerat, Spectromet, Detect Assoc Equip 1997;397(2–3):478–82.
[3] Oka Y et al. Gamma-ray spectrometric study of the photoactivation products with 20 MeV bremsstrahlung. J Nucl Sci Technol 1967;4(7):346–52.
[4] Bosch H, Munczek H. New half-life in the family of antimony isotopes. Phys Rev 1957;106(5):983–5.
[5] Siegel JM, Glendenin LE. Radiochemical studies: the fission products. National nuclear energy series IV. New York: McGraw-Hill; 1951.
[6] Gross JL, Thoennessen M. Discovery of gallium, germanium, lutetium, and hafnium isotopes. Atom Data Nucl Data Tables 2012;98(5):983–1002.
[7] Li Y et al. New levels and transitions in 72 Ge following the decay of 72 Ga. Chin Phys 2005;14(1):95.
[8] Moreh R, Shahal O. Use of the (γ, γ′) reaction for studying the energy levels of 75As. Phys Rev 1969;188(4):1765–70.
[9] Ng A et al. Gamma rays from the decay of 75Ge and 77Ge. Phys Rev 1968;176(4):1329–38.
[10] McCarthy JJ. A systematic study of the photo-disintegration of germanium isotopes in Physics and Astronomy. Iowa State University: Digital Repository @ Iowa State University; 1973. p. 114. <http://lib.dr.iastate.edu/>.
[11] Lin M et al. Near-infrared light activated delivery platform for cancer therapy. Adv Colloid Interface Sci 2015;226(Part B):123–37.
[12] Wagner CD. The cadmium photoactivation dosimeter. Int J Appl Radiat Isotopes 1965;16(11):645–8.
[13] Hugtenburg RP. Microdosimetry in X-ray synchrotron based binary radiation therapy. Eur J Radiol 2008;68(Suppl. 3):S126–8.
[14] Hugtenburg RP, Baker AER, Green S. X-ray synchrotron microdosimetry: experimental benchmark of a general-purpose Monte Carlo code. Appl Radiat Isotopes 2009;67(3):433–5.
[15] Cheng M-K et al. Photoradiation therapy: current status and applications in the treatment of brain tumors. Surg Neurol 1986;25(5):423–35.
[16] Krmar M et al. Endpoint energy of linear medical accelerators. Nucl Instrum Methods Phys Res Sect A: Accelerat, Spectromet, Detect Assoc Equip 2004;532(3):533–7.
[17] Aizatskiy NI et al. Carrier-free production of 95Tc at an electron accelerator. Nucl Instrum Methods Phys Res Sect B: Beam Interact Mater Atoms 2011;269(24):3125–8.
[18] Garzón OL, Rocco GG. Photoproduction of 7Be from natural boron and beryllium. J Inorgan Nucl Chem 1967;29(1):1–6.
[19] Kneissl U. Photoactivation and photon-scattering experiments of astrophysical relevance. Prog Particle Nucl Phys 2001;46(1):79–88.
[20] von Neumann-Cosel P et al. Photoactivation of 180Tam and s-process nucleosynthesis of nature's rarest naturally occurring isotope. Nucl Phys A 2001;688(1–2):237–40.
[21] Vogt K et al. Determination of (γ, n) reaction rates for the astrophysical γ process. Nucl Phys A 2003;718:575–7.
[22] Mohr P et al. Photoreactions in nuclear astrophysics. Nucl Phys A 2003;718:243–6.
[23] Vogt K et al. Measurement of the (γ, n) cross section of the nucleus 197Au close above the reaction threshold. Nucl Phys A 2002;707(1–2):241–52.
[24] Zilges A, Mohr P. Reactions with real photons in the vicinity of the neutron threshold. Prog Particle Nucl Phys 2000;44:39–48.
[25] Dillmann I et al. Solving the stellar 62Ni problem with AMS. Nucl Instrum Methods Phys Res Sect B: Beam Interact Mater Atoms 2010;268(7–8):1283–6.
[26] Utsunomiya H et al. Direct determination of photodisintegration cross sections and the p-process. Nucl Phys A 2006;777:459–78.
[27] Ridikas D et al. Status of the photonuclear activation file: Reaction cross-sections, fission fragments and delayed neutrons. Nucl Instrum Methods Phys Res Sect A: Accelerat, Spectromet, Detect Assoc Equip 2006;562(2):710–3.
[28] Otvos JW et al. Photoactivation and photoneutron activation analysis. Nucl Instrum Methods 1961;11:187–95.
[29] Tazawa E, Fujiwara A, Yasumasu I. Activation of co-insensitive respiration in echiuroid eggs by light irradiation at various wavelengths. Comparat Biochem Physiol Part B: Comparat Biochem 1991;99(1):207–11.
[30] Bencardino R et al. Efficient Monte Carlo simulation of delayed activation analysis experiments. Nucl Instrum Methods Phys Res Sect B: Beam Interact Mater Atoms 2010;268(5):513–8.
[31] Tustonić T et al. Photoactivation of isomeric level in 115In. Appl Radiat Isotopes 1997;48(1):45–9.
[32] Wesolowski JJ et al. Energy levels of 31S and 19Ne. Nucl Phys 1965;71(3):586–92.
[33] Hamburger EW, Hamburger AI. Energy levels of Y90 from the Y89 (d, p)Y90 reaction. Nucl Phys 1965;68(1):209–20.
[34] Brown G, MacGregor A, Middleton R. Level structure measurements with the (p, α) reaction: (II). Energy levels of 47V and 49V. Nucl Phys 1966;77(2):385–93.
[35] Krane KS. The decays of 70,72Ga to levels of 70,72Ge and the neutron capture cross sections of 69,71Ga. Appl Radiat Isotopes 2012;70(8):1649–57.
[36] Ythier C et al. The decay of 73Ga. Nucl Phys 1958;9(1):108–15.
[37] Bošnjaković B, Van Best JA, Bouwmeester J. Energy levels of 38Ar from the 37Cl (p, α0)34S reaction. Nucl Phys A 1967;94(3):625–52.
[38] Ajzenberg-Selove F, Bingham HG, Garrett JD. Energy levels of 14C. Nucl Phys A 1973;202(1):152–60.
[39] Kent JJ, Blatt SL. Energy levels of 92Nb and 94Tc from 92Zr, 94Mo(p, nγ)92Nb, 94Tc. Nucl Phys A 1975;255(2):296–306.
[40] Pougheon F et al. First study of the (14C, 12C) reaction: Selectivity of the reaction and the energy levels of 28Mg and 30Si. Nucl Phys A 1981;355(1):207–20.
[41] Tilley DR et al. Energy levels of light nuclei. Nucl Phys A 2004;745(3–4):155–362.
[42] Mohr P et al. Photoactivation at a clinical LINAC: the reaction slightly above threshold. Nucl Instrum Methods Phys Res Sect A: Accelerat, Spectromet, Detect Assoc Equip 2007;580(3):1201–8.
[43] Kapitza SP, Tsipenyuk YM. Trends in electron accelerator applications. Nucl Instrum Methods Phys Res Sect B: Beam Interact Mater Atoms 1998;139(1–4):1–11.
[44] Anderson JA et al. Nuclear activation techniques for measuring direct and backscattered components of intense bremsstrahlung pulses. Nucl Instrum Methods Phys Res Sect B: Beam Interact Mater Atoms 1989;40:1189–92.
[45] Larsson B, Stepanek J. Future electron accelerators and free electron lasers: potentials in clinical medicine. Nucl Instrum Methods Phys Res Sect A: Accelerat, Spectromet, Detect Assoc Equip 1997;398(1):85–9.
[46] Accelerator ED. Technical Training Guide; 2003.
[47] ORTEC. MAESTRO 32. In: MCA-Emulation-Software; 2012.
[48] Radford D. RadWare. Oak Ridge National Laboratory: Physics Division, Oak Ridge National Laboratory.
[49] Khazov Y, Rodionov A, Kondev FG. Nuclear data sheets for A = 133. Nucl Data Sheets 2011;112(4):855–1113.
[50] Blachot J. Nuclear data sheets for A = 109. Nucl Data Sheets 2006;107(2):355–506.
[51] Bhat MR. Nuclear data sheets for A = 57. Nucl Data Sheets 1998;85(3):415–536.
[52] Browne E, Tuli JK. Nuclear data sheets for A = 60. Nucl Data Sheets 2013;114(12):1849–2022.
[53] Browne E, Tuli JK. Nuclear data sheets for A = 137. Nucl Data Sheets 2007;108(10):2173–318.
[54] Dong Y, Junde H. Nuclear data sheets for A = 54. Nucl Data Sheets 2014;121:1–142.
[55] Basunia MS. Nuclear data sheets for A = 22. Nucl Data Sheets 2015;127:69–190.

[56] Wu SC. Nuclear data sheets for A = 214. Nucl Data Sheets 2009;110 (3):681–748.
[57] Shamsuzzoha Basunia M. Nuclear data sheets for A = 210. Nucl Data Sheets 2014;121:561–694.
[58] Abusaleem K. Nuclear data sheets for. Nucl Data Sheets 2014;116: 163–262.
[59] Martin MJ. Nuclear data sheets for A = 208. Nucl Data Sheets 2007;108 (8):1583–806.
[60] Gun AM, Gupta MK, Dasgupta B. Fundamentals of statistics. World Press; 2008.
[61] Wasserman L. All of statistics: a concise course in statistical inference. Springer; 2004.
[62] Feller W. An introduction to probability theory and its applications. Wiley; 1971.
[63] Taboga M. Lectures on probability theory and mathematical statistics. 2nd ed. CreateSpace Independent Publishing Platform; 2012.
[64] Negret A, Singh B. Nuclear data sheets for A = 75. Nucl Data Sheets 2013;114 (8–9):841–1040.
[65] Nesaraja CD. Nuclear data sheets for A=69. Nucl Data Sheets 2014;115:1–134.